Supplementary Information (SI) for Inorganic Chemistry Frontiers.
This journal is © the Partner Organisations 2024

Supplementary information

Boosted Aluminum Storage Performance by d-p Orbital Modulation in Zinc Selenide with Manganese Element Dopants

Experimental section

Material synthesis

Synthesis of ZIF-8: ZIF-8 was fabricated on the basis of a previous work.[1] 1.59 g $Zn(NO_3)_2 \cdot 6H_2O$ and 1.32 g 2-methylimidazole were completely dissolved into 120 ml methanol, respectively, to form solution A and B. Then solution B was slowly added into solution A under vigorously stirring for 15 min. After that, the mixture solution was transferred into a flask and heated at 60 ℃ for 12 h. Finally, the white precipitation was centrifuged and washed with anhydrous ethanol for several times and dried at 60 ℃ for 12h to obtain ZIF-8.

Synthesis of Mn-ZIF-8: 1g of the as-prepared ZIF-8 was ultrasonically dispersed in 100ml methanol containing 2 mmol $(CH_3COO)_2Mn \cdot 4H_2O$ and was stirred for 4 h to adsorb Mn species completely. Then the Mn-ZIF-8 sample was acquired by washing with anhydrous ethanol three times and dried at 60 ℃ for 12h. In comparison, we also prepared Mn0.4-ZIF-8 and Mn4-ZIF-8 samples by changing the content of $(CH_3COO)_2Mn \cdot 4H_2O$ to 0.4 mmol and 4 mmol under same condition.

Synthesis of Mn-ZnSe@CNPC: 3 g $C_3H_4N_6$ was put into muffle furnace and heated at 550 ℃ for 4 h to obtain g-C_3N_4. Then 1 g of Mn-ZIF-8 and 0.5 g of g-C_3N_4 were thoroughly ball milled in an Ar atmosphere. The as-prepared mixture and selenium powder with a mass ratio of 1:2 was placed in the middle and upstream of the tube furnace and heated at 650 ℃ for 2 h with a ramp rate of 5 ℃ min^{-1} under Ar atmosphere to obtain Mn-ZnSe@CNPC. As the reference, ZnSe@PC sample was prepared without the introduction of Mn-ion and g-C_3N_4, and ZnSe@CNPC sample without Mn-ion.

Electrochemical measurement

80 wt% as-prepared active material, 10 wt% acetylene black, 10 wt% polyvinylidenedifluoride were combined in N-methyl-pyrrolidone and stirred for 24 hours to obtain a uniform slurry. The slurry was

uniformly cast on Mo foil (20 μm thickness, 99.99%) and dried in vacuum oven at 60 °C overnight. The mass loading of the cathode material was about 1 mg cm^{-2}. An ionic liquid electrolyte of $AlCl_3$/1-ethyl-3-methylimidazolium chloride ([EMIm]Cl) with a molar ratio of 1.1:1 was utilized. The aluminum foil and Whatman glass microfiber filters (GF/A) were used as anode and separator. The Swagelok-type cells (**Fig. S1**) were assembled to test the electrochemical properties of RABs. The galvanostatic charge/discharge and galvanostatic intermittent titration (GITT) measurements were performed on the Land CT2001A system between 0.01–1.8 V. An electrochemical workstation (CHI 660E) was used to perform cyclic voltammetry (CV) and electrochemical impedance spectroscopy (EIS) tests.

Materials characterization

Scanning electron microscopy (SEM) images were acquired using a Zeiss Gemini 500 microscope with an accelerated voltage of 5 kV. Transmission electron microscopy (TEM) images were captured using a JEOL JEM F200 microscope. X-ray diffraction (XRD) patterns were obtained using a Bruker D8 X-ray diffractometer (Germany) with Cu-K_α radiation. X-ray photoelectron spectroscopy (XPS) measurements were performed using a Thermo SCIENTIFIC ESCALAB 250Xi (America). The Raman spectra were performed using a HORIBA XploRA Nano (Switzerland). Brunauer-Emmett-Teller surface area tests were implemented using Quantachrome Autosorb-IQ-MP.

Theoretical calculation

First-principles calculations are based on density-functional theory (DFT) without the Projector Augmented Wave (PAW) method and are performed using the Vienna *ab initio* simulation package (VASP). The energy cutoff was set to 330 eV, and the *k*-points mesh of Brillouin-zone was selected as 2 × 2 × 1. The force-convergence criterion for ion relaxation was 0.02 eV/Å and the energy-

convergence criterion for electron self-consistency was 10^{-5} eV. The (111) plane of ZnSe was cut using Atom Simulation Environment (ASE) for the adsorption of $AlCl_4^-$.

Equation S1, **S2,** and **S3** to ascertain aluminum ion diffusion kinetics.

$$\omega = 2\pi f \quad \textbf{S1}$$

$$D = \frac{R^2T^2}{2A^2n^4F^4C^2\sigma^2} \quad \textbf{S2}$$

$$Z` = R_{ct} + R_e + \sigma\omega^{-1/2} \quad \textbf{S3}$$

where D is the diffusion coefficient of Al^{3+}, R and T refer to the gas constant and absolute temperature, respectively, A represents the area of the positive electrode, n represents the number of electrons transferred per mole of substance in the redox reaction, F represents the Faraday constant, C represents the concentration of Al^{3+} in the electrode, σ is the Warburg factor, and ω is the angular velocity.

Equation S4 to calculating aluminum-ion diffusion coefficients by GITT tests.

$$D = \frac{4}{\pi\tau}\left(\frac{m_bV_m}{M_bS}\right)^2\left(\frac{\Delta E_s}{\Delta E_\tau}\right)^2 \quad \textbf{S4}$$

where τ, m_b, V_m, M_b, and S represent relaxation time, mass, molar volume, molar mass, and electrode area, respectively. The ΔE_s and ΔE_τ are voltage variations occurring in relaxation steps and the current pulse.

Equation S5 to calculating the theoretical capacity of ZnSe.

$$\text{Capacity (theory)} = \frac{nF}{3.6M_w}\ \text{mAh g}^{-1} \quad \textbf{S5}$$

where the n, F, M_w represent the number of electrons transferred per mole of electrode materials in the redox reaction, Faraday constant, molar mass of electrode materials.

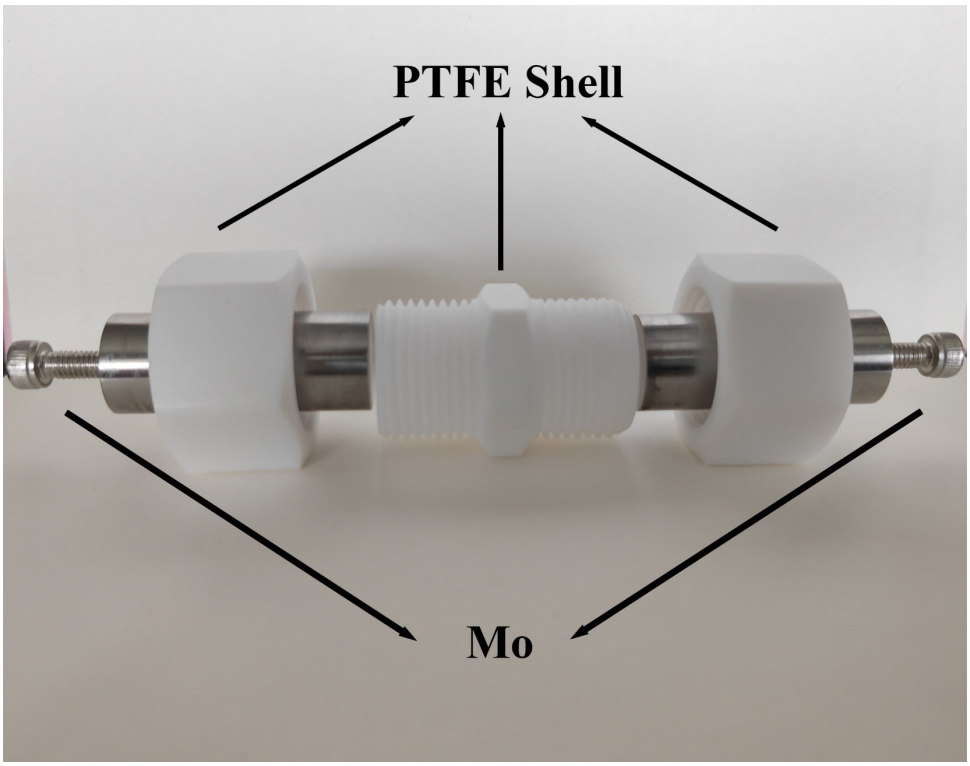

Fig. S1. Digital photograph of Swagelok-type cell.

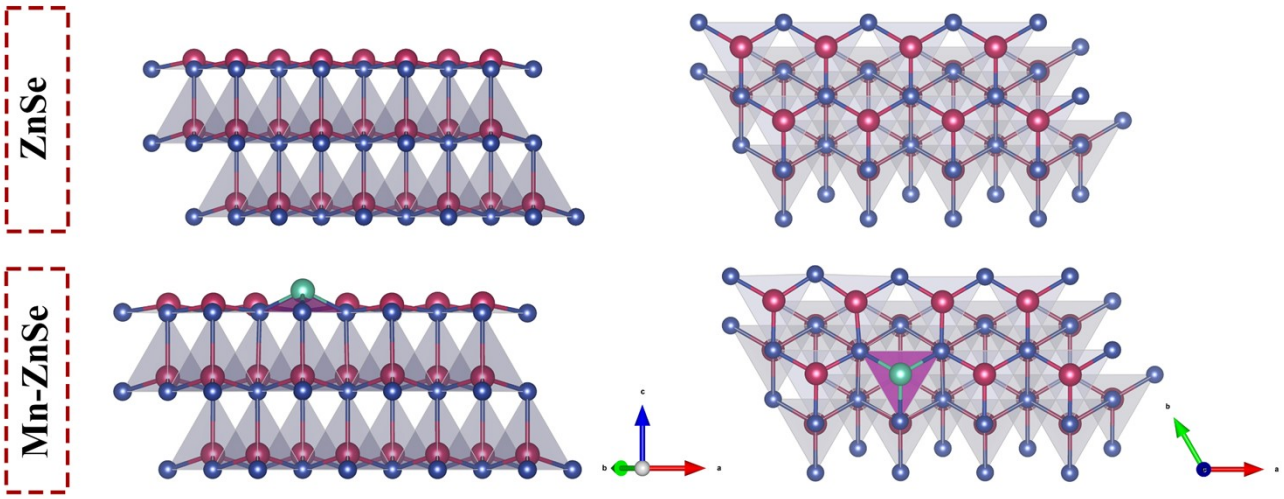

Fig. S2. Optimized structures of ZnSe and Mn-ZnSe.

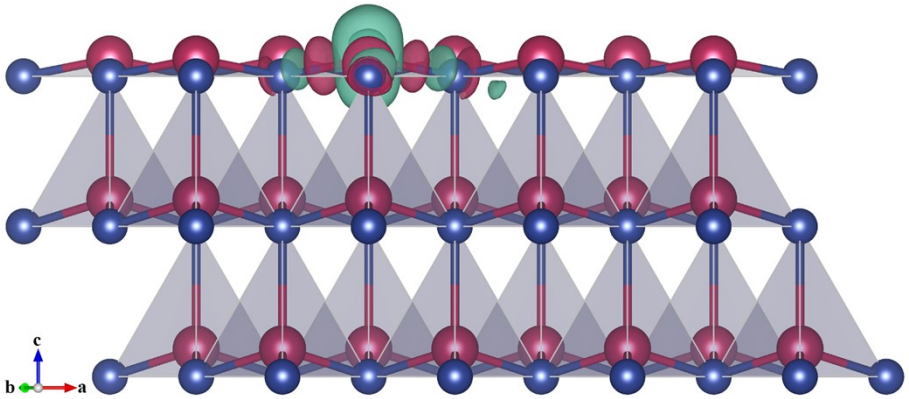

Fig. S3. Differential charge density distribution of ZnSe.

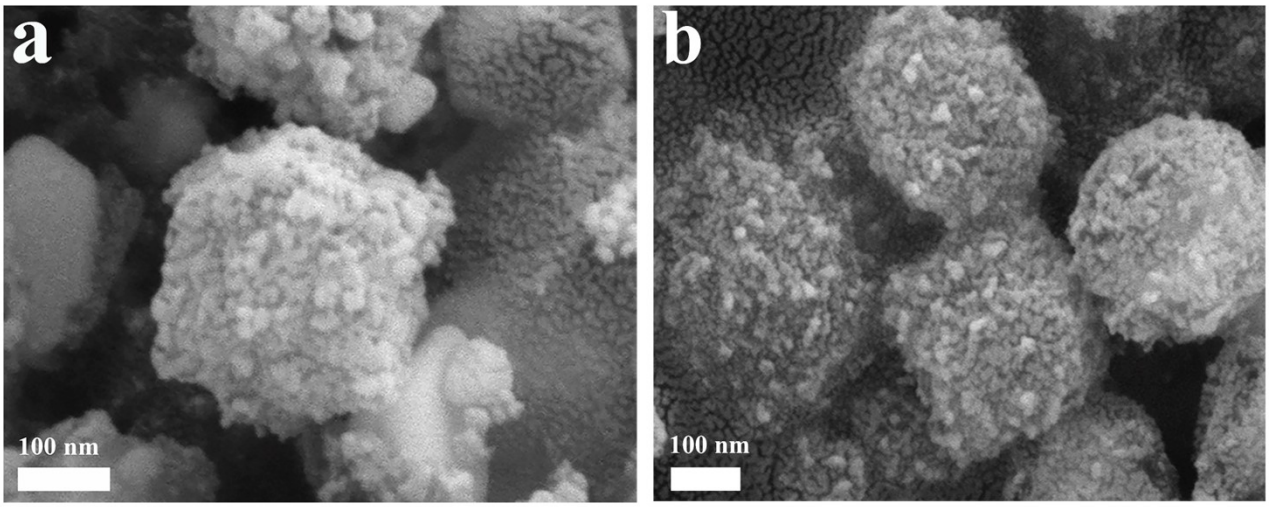

Fig. S4. SEM images of (a) ZnSe@CNPC and (b) ZnSe@PC.

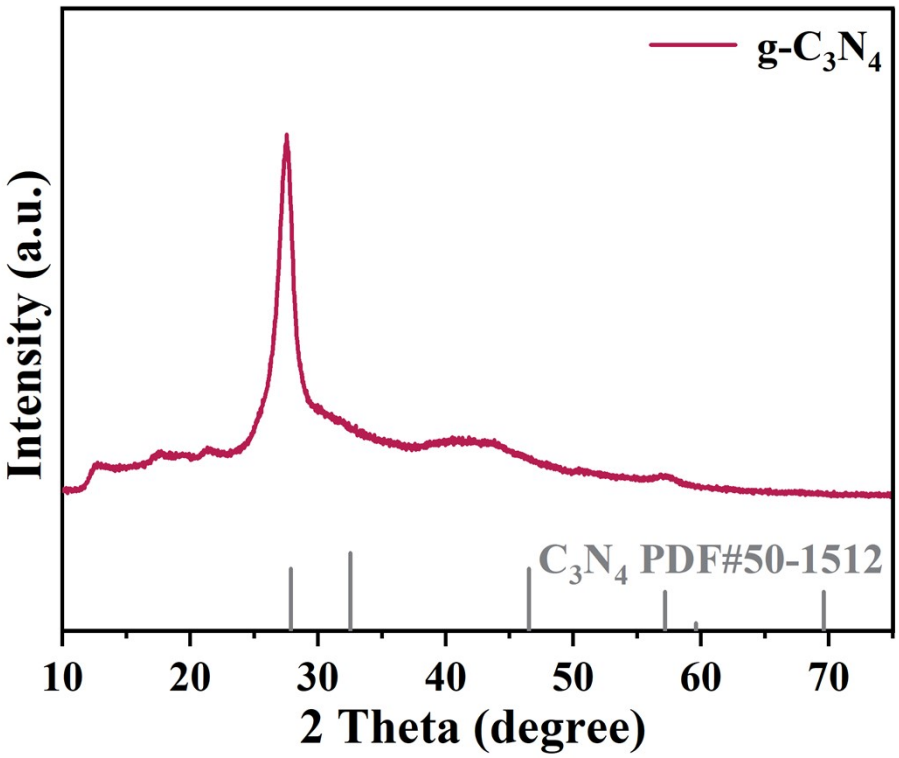

Fig. S5. The XRD spectra and standard cards of pure g-C_3N_4.

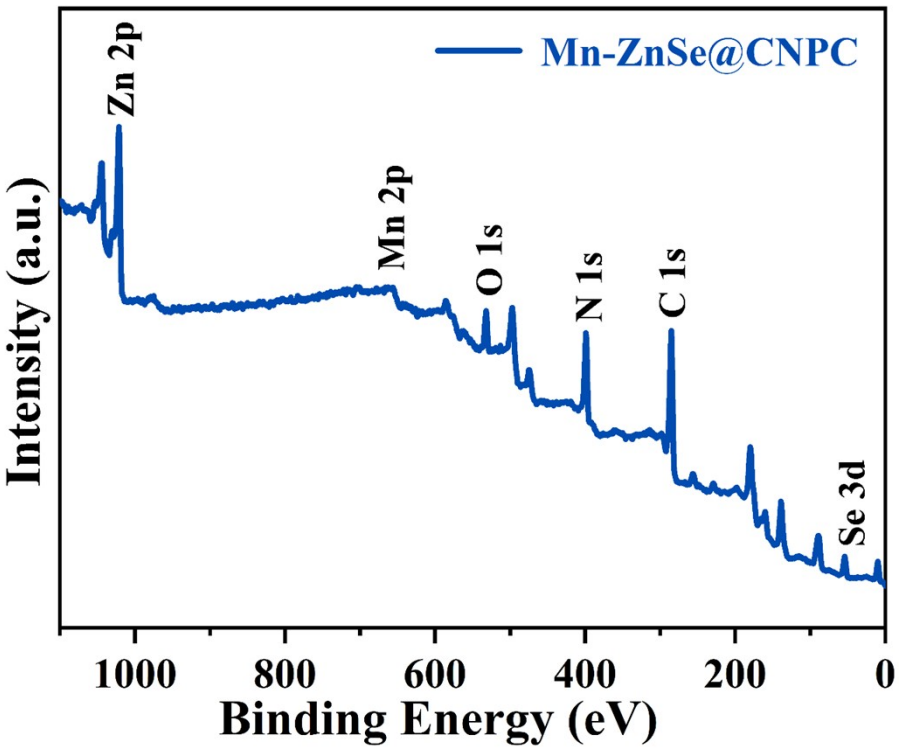

Fig. S6. XPS survey spectrum of Mn-ZnSe@CNPC.

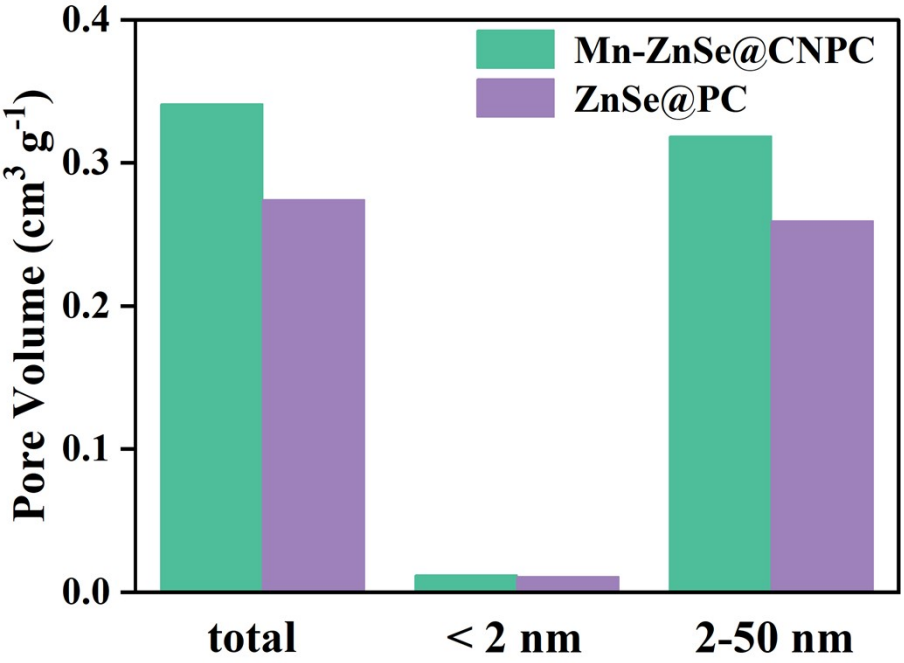

Fig. S7. The pore volume of Mn-ZnSe@CNPC and ZnSe@PC.

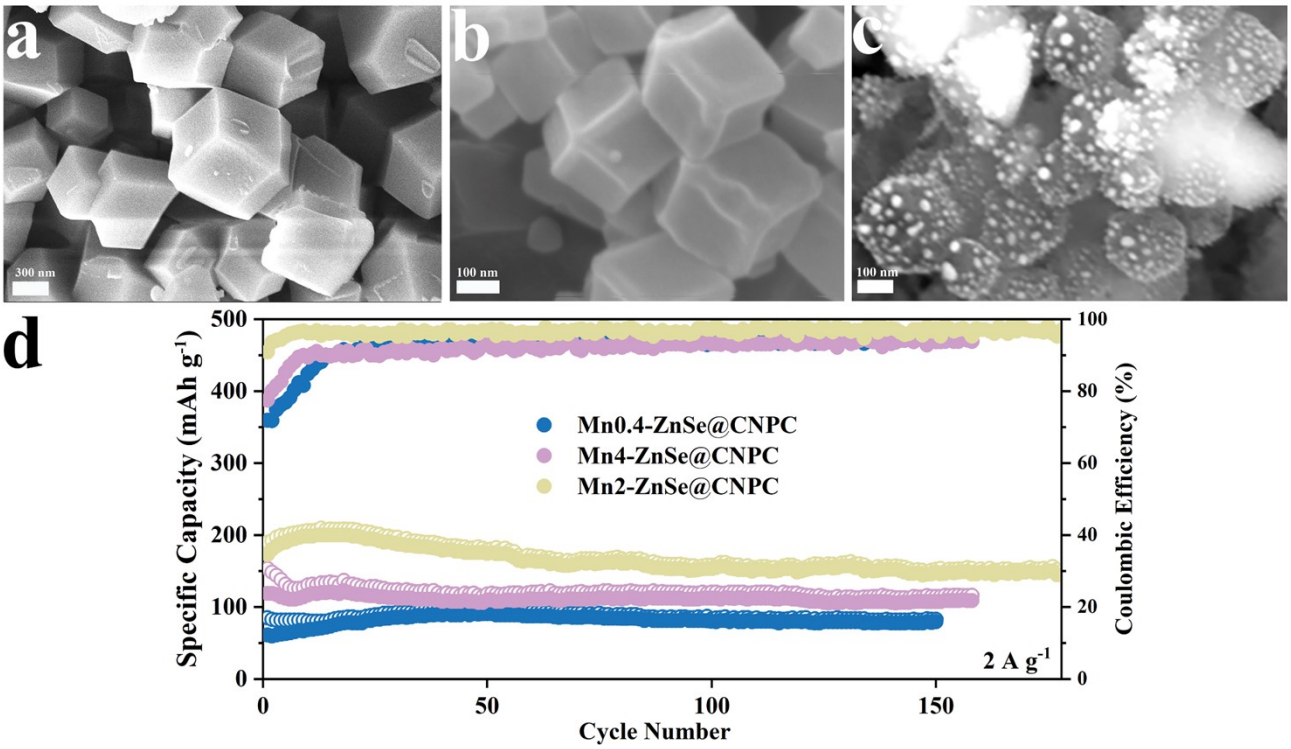

Fig. S8. SEM images of (a) Mn0.4-ZIF-8, (b) Mn2-ZIF-8, and (c) Mn4-ZIF-8. (d) The cycling performance of Mn0.4-ZnSe@CNPC, Mn2-ZnSe@CNPC, and Mn4-ZnSe@CNPC cathodes at 2 A g^{-1}.

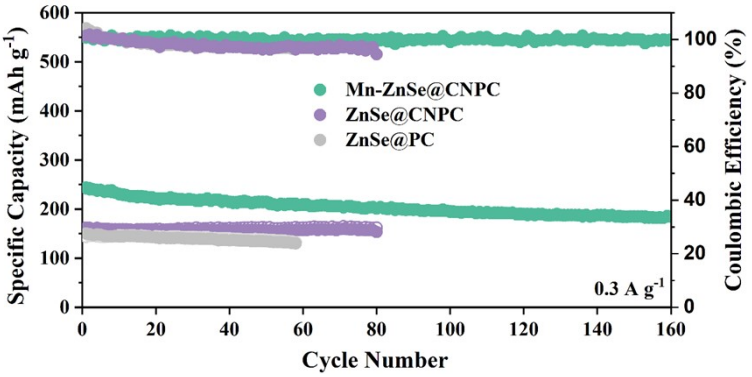

Fig. S9. The cycling performance of Mn-ZnSe@CNPC, ZnSe@CNPC, and ZnSe@PC cathodes at 0.3 A g^{-1}.

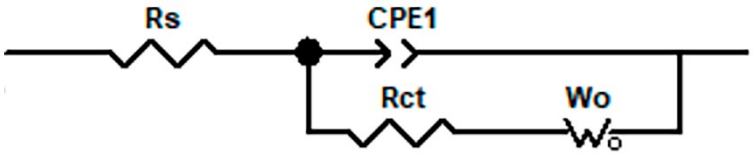

Fig. S10. The fitted equivalent circuit diagram of EIS tests.

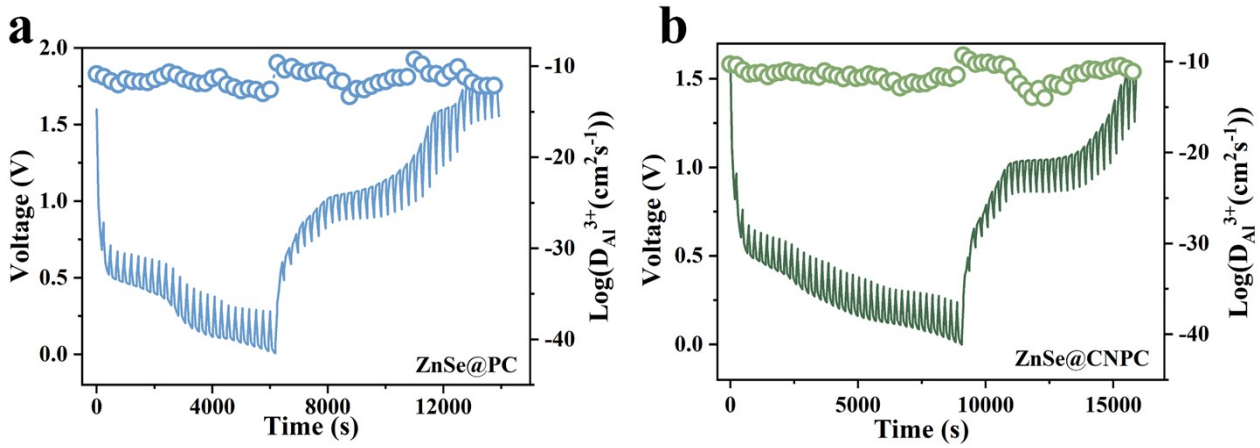

Fig. S11. GITT curve for (a) ZnSe@PC and (b) ZnSe@CNPC cathodes.

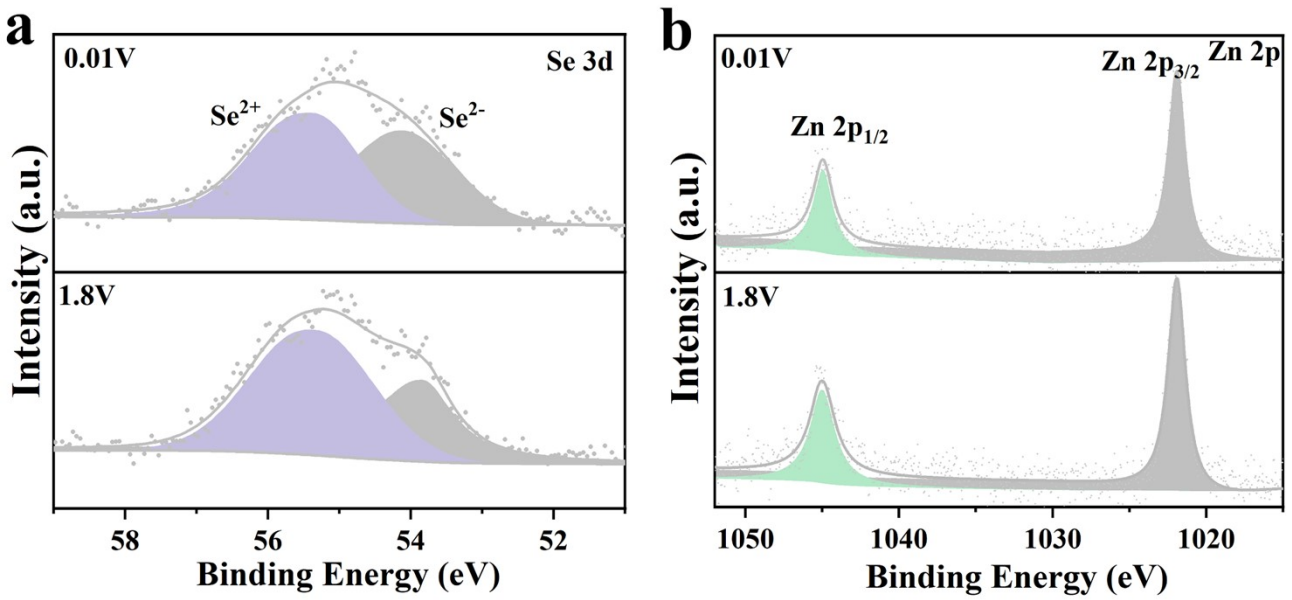

Fig. S12. The *ex situ* XPS spectra of (a) Se 3d and (b) Zn 2p peaks for Mn-ZnSe@CNPC electrode at 0.01 V and 1.8 V.

	Standard ZnSe phase	Mn-ZnSe@CNPC
a (Å)	5.6676	5.6692
b (Å)	5.6676	5.6692
c (Å)	5.6676	5.6692
α (°)	90	90
β (°)	90	90
γ (°)	90	90
Space group	F -4 3 m	F -4 3 m
χ^2		2.42
R_{wp}		7.13

Table S1. The refined XRD results of Mn-ZnSe@CNPC and the standard cell parameters of ZnSe phase.

Strategy	Capacity (mAh g^{-1})	Current density (A g^{-1})	Cycle (number)	Reference
$NiSe_2$	52	1	250	[2]
Co_3S_4	150	0.05	92	[3]
CuS@C	90	0.02	100	[4]
SnSe	107	0.3	100	[5]
δ-MnO_2	37	0.1	100	[6]
G-SnS_2	70	0.2	100	[7]
VS_4/rGO	60	0.3	100	[8]
graphite flakes	100	0.6	300	[9]
S–NiCo@rGO	83	1	100	[10]
Cu_3P	147	0.05	50	[11]
V_2CT_x MXene	90	0.1	100	[12]
SnSe	107	0.3	100	[13]
CoSe	5	63	100	[14]
Ni_3S_2@Graphene	60	0.1	100	[15]
Mn-ZnSe@CNPC	**150** **90** **185**	**2** **3** **0.3**	**200** **1300** **160**	**This work**

Table S2. Comparison of electrochemical performance of Mn-ZnSe@CNPC electrodes with state-of-the-art cathode materials.

Notes and References

1 P. Zhan, F. Hu, L. Long, J. Chen, Y. Chai, W. Sun, C. Wang and X. Peng, Mechanistic and structure investigation of the KOH activation ZIF-8 derived porous carbon as metal-free for unprecedented peroxymonosulfate activation degradation of bisphenol A, *Chemosphere*, 2022, **307**, 135961.

2 H. Zhang, Y. Liu, L. Yang, L. Zhao, X. Dong, H. Wang, Y. Li, T. Sun, Q. Li and H. Li, A highly reversible Co3S4 microsphere cathode material for aluminum-ion batteries, *Energy Storage Materials*, 2022, **47**, 336–344.

3 H. Li, H. Yang, Z. Sun, Y. Shi, H.-M. Cheng and F. Li, High-Performance Aluminum-Ion Battery with CuS@C Microsphere Composite Cathode, *Nano Energy*, 2019, **56**, 100–108.

4 S. Wang, S. Jiao, J. Wang, H.-S. Chen, D. Tian, H. Lei and D.-N. Fang, SnSe nano-particles as advanced positive electrode materials for rechargeable aluminum-ion batteries, *ACS Nano*, 2017, **11**, 469–477.

5 Y. Zhang, B. Zhang, J. Li, J. Liu, X. Huo and F. Kang, δ-MnO2 Nanofibers: A Promising Cathode Material for New Aluminum-Ion Batteries, *Chemical Engineering Journal*, 2021, **403**, 126377.

6 P. Almodóvar, D. A. Giraldo, J. Chancón, I. Álvarez-Serrano and M. L. López, An Innovative Freeze-Dried Reduced Graphene Oxide Supported SnS2 Cathode Active Material for Aluminum-Ion Batteries, *ChemElectroChem*, 2020, **7**, 2102–2106.

7 Y. Hu, B. Luo, D. Ye, X. Zhu, M. Lyu and L. Wang, Flower-like Vanadium Suflide/Reduced Graphene Oxide Composite: An Energy Storage Material for Aluminum-Ion Batteries, *Advanced Materials*, 2017, **29**, 1606132.

8 X. Zhang, S. Wang, J. Tu, G. Zhang, S. Li, D. Tian and S. Jiao, Binder-free ultrasonicated graphite flakes@carbon fiber cloth cathode for rechargeable aluminum-ion battery, *ChemSusChem*, 2018, **11**, 709–715.

9 C. Liu, Z. Liu, Q. Li, H. Niu, C. Wang, Z. Wang and B. Gao, Layered double hydroxides derived NiCo-sulfide as a cathode material for aluminum ion batteries, *Journal of Power Sources*, 2019, **438**, 226950.

10 W. Xing, X. Li, T. Cai, Y. Zhang, P. Bai, J. Xu, H. Hu, M. Wu, Q. Xue, Y. Zhao, J. Zhou, S. Zhuo, X. Gao and Z. Yan, *Electrochimica Acta*, 2020, **344**, 136174.

11 G. Li, J. Tu, M. Wang and S. Jiao, *J. Mater. Chem. A*, 2019, **7**, 8368–8375.

12 A. VahidMohammadi, A. Hadjikhani, S. Shahbazmohamadi and M. Beidaghi, *ACS Nano*, 2017, **11**, 11135–11144.

13 Y. Zhang, B. Zhang, J. Li, J. Liu, X. Huo and F. Kang, *Chemical Engineering Journal*, 2021, **403**, 126377.

14 W. Xing, D. Du, T. Cai, X. Li, J. Zhou, Y. Chai, Q. Xue and Z. Yan, *Journal of Power Sources*, 2018, **401**, 6–12.

15 S. Wang, Z. Yu, J. Tu, J. Wang, D. Tian, Y. Liu and S. Jiao, *Advanced Energy Materials*, 2016, **6**, 1600137.